Korean J. Chem. Eng., **28**(1), 184-188 (2011)
DOI: 10.1007/s11814-010-0314-4

Formation of abnormally large-sized tubular amyloid β aggregates on a nanostructured gold surface

Jeongjin Lee*, Junsu Park*, Byoung Kyu Kwak*, Inhee Choi*, Younghun Kim, Kyunghee Choi***, and Jongheop Yi*,†**

*School of Chemical and Biological Engineering, Institute of Chemical Processes, Seoul National University, Seoul 151-742, Korea
**Department of Chemical Engineering, Kwangwoon University, Wolgye-dong, Nowon-gu, Seoul 139-701, Korea
***National Institute of Environmental Research, Incheon 404-708, Korea
(*Received 6 March 2010 • accepted 28 April 2010*)

Abstract–The effect of the properties of a nanostructured gold surface (nano-Au surface) on the aggregation of Amyloid β(1-40) (Aβ40) was investigated. A nano-Au surface, in the form of immobilized nanoparticles, was prepared by using a thermal evaporator, resulting in the formation of nanosized clusters with sizes less than 10 nm. When Aβ40 was incubated with the nano-Au surface, abnormally large-sized tubular aggregates were formed on the surface and typical fibril formation was suppressed in the solution. This abnormally large tubular structure represents a novel type of Aβ40 aggregate. In the absence of the nano-Au surface, the diameters of the Aβ40 fibrils were less than 10 nm. However, the height of the tubular aggregates formed on a nano-Au surface was 80-100 nm. Such large-sized aggregates of Aβ40 have not been reported in previous studies dealing with interactions of suspended nanoparticles with proteins. This can be attributed to differences in the aggregation mechanism between immobilized and suspended nanoparticles. The formation of Aβ40 aggregates by nano-Au surface will provide the possible mechanism for abnormal fibril formation.

Key words: AFM, Amyloid β40, Fibril, Nano-Au Surface, Protein Aggregation

INTRODUCTION

With the current applications of nanotechnology in medical science, an understanding of the specific interactions that occur between proteins and nanomaterials is an important issue in the areas of nanomedicine and nanosafety [1,2]. When nanomaterials come into contact with proteins, the nanomaterial can have an effect on the behavior of a protein. In this context, the effect of a nanomaterial on the aggregation of amyloidogenic proteins has been a subject of considerable interest, in terms of understanding the various etiological relationships between this and neurodegenerative diseases such as Alzheimer's, Parkinson's and dialysis-related amyloidosis [3]. It was recently reported that the kinetics of the protein aggregation *in vitro* are affected by the presence of nanomaterials. For example, copolymeric nanoparticles accelerate the aggregation of β-2-microglobulin [4] and gold nanoparticles initiate the formation of lysozyme aggregates in the physiological pH range, resulting in the formation of extended assemblies of amorphous protein-nanoparticles [5]. Even for an identical amyloid protein, the kinetics of aggregation appears to depend on the type of nanoparticle present. TiO_2 nanoparticles promote the formation of Amyloid β fibrils [6], but copolymeric nanoparticles [7] and biocompatible nanogels [8] act as inhibitors. A possible mechanism for this is as follows [4]. In the first step, the protein binds to the surface of nanoparticles. This binding results in a subsequent increase in the concentration of the protein in the vicinity of the nanoparticle surface. This would increase the probability of a morphological change, followed by an acceleration in the aggregation of the protein [4-6] or it could result in monomer depletion and the trapping of sub- and near-critical nuclei, followed by the inhibition of aggregation [7].

Herein, the effect of a nanostructured gold surface (nano-Au surface), as an immobilized form of nanoparticles, on the change in aggregation properties of Amyloid β40 (Aβ40) was examined as shown in Fig. 1(a). Suspensions of nanoparticles have been typically used in previous studies concerning the role of nanomaterials

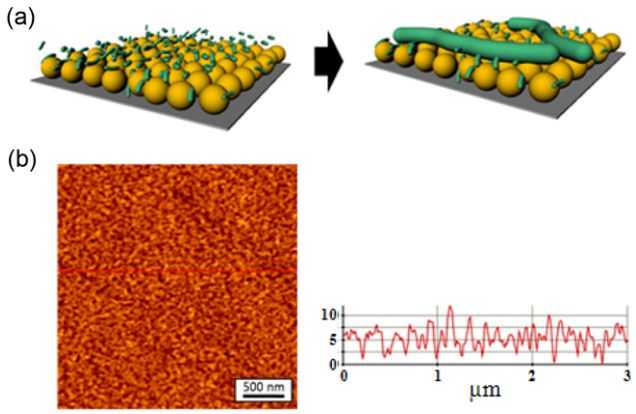

Fig. 1. Schematic image of the formation of large size Aβ40 aggregates on a nanostructured gold surface (a) and AFM images of a nanostructured gold surface showing that the size of the clusters are under 10 nm (b); The right is the line profile from an AFM image.

†To whom correspondence should be addressed.
E-mail: jyi@snu.ac.kr

on protein aggregation, and the focus has been on the kinetics of fibril formation. In contrast, we employed an immobilized form of nanoparticles and focused our attention on morphological variations on the surface as well as the kinetics associated with aggregation. The morphological change of Aβ40 on the surface was visualized by an atomic force microscopy (AFM). In addition, using this approach, it is possible to withdraw samples of Aβ40 aggregates from the solution, which is separated from the aggregates on the surface, for quantitative analysis. In experiments using suspensions of nanoparticles, an analysis of morphological changes of the surface and aggregates that are not bound to the nanoparticle surface, i.e., in solution, is a difficult task. Using the approach described herein, we were able to independently detect changes on the nanostructured surface via AFM and those in bulk solution via the use of a time-resolved thioflavin T (ThT) binding assay and transmission electron microscope analysis.

EXPERIMENTAL

1. Materials

Aβ40 treated by hexafluoroisopropanol (HFIP) [10] was purchased from rPeptide (U.S.A). A solution of Aβ40 was prepared according to a previously described method [11].

2. Sample Preparation

Nano-Au surfaces were prepared by using a thermal evaporator (MHS-1800, Moohan Vacuum Co.), permitting a thin Au layer to be deposited on clean glass slides (SF10, 25×15 mm^2). The formation of nanosized clusters (<10 nm, Fig. 1(b)) was confirmed by AFM. A 10 μM aliquot of Aβ40 was incubated at 37 °C in 20 μM sodium phosphate buffer (pH 7.4) in the absence and presence of a nano-Au surface. Contact between the Aβ40 and the nano-Au substrate was achieved by immersing the two substrates in solution without agitation. A thioflavin T binding assay was conducted during the incubation. After exposure for 24, 48, 72 and 96 h, the substrates were removed from the Aβ40 solution and the surface was examined by *ex-situ* atomic force microscopy, as follows. All substrates were incubated on a continuous basis. Namely, the surface examined by ex-situ AFM was not immersed in the Aβ40 solution for further contacting.

3. Thioflavin T Binding Assay

Because thioflavin T is known to associate rapidly with fibrils and protofibrils, giving rise to enhanced emission at around 482 nm, a fluorescence assay with a fluorescence spectrometer can be used to monitor the appearance and growth of fibrils [12]. Two hundred μl aliquots from the tubes were removed at different time points and added to 2 ml of a solution of Thioflavin T (10 μM) in a cuvette with a 10 mm path length. The fluorescence was measured at 482 nm (silt 5 nm) with excitation at 440 nm (silt 5 nm) with a Perkin Elmer LS55 Spectrophotometer (PerkinElmer Ltd., Beaconsfield, UK) equipped with a xenon lamp. This measurement was replicated a total of three times, and the average value was calculated from the three replicates.

4. Atomic Force Microscope

The topographical images of the Aβ40 aggregates were measured by using an AFM apparatus (PSIA, XE-100, Korea) in the contact mode, using a silicon cantilever with a typical tip curvature radius of 10 nm (NSC36 series, MikroMasch, Estonia). The force constant and resonance frequency were 0.45 N/m and 95 kHz, respectively. A force/distance curve was also obtained in the AFM experiments to distinguish between the deposited materials.

5. Transmission Electron Microscopy

The Aβ40 aggregates in solution were observed by transmission

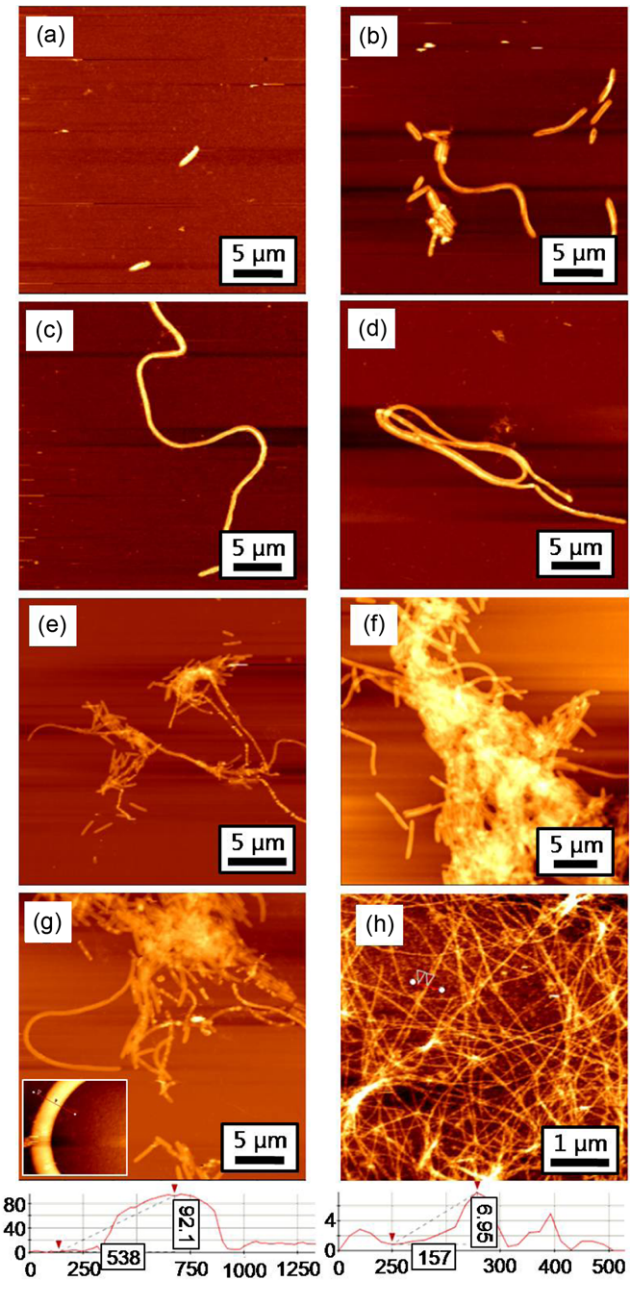

Fig. 2. Representative AFM images of Aβ40 assemblies on the surface of nanostructured gold substrates ((a)-(g)) and in solution in the absence of substrates (h). The substrates were incubated in 10 μM Aβ40 at 37 °C for 48 hr (a), 72 hr (b)-(d), and 96 hr (e)-(g), followed by an analysis of the surface by AFM. To detect the assemblies of Aβ40 in solution, aliquots from the solution in the presence and absence of nano-Au substrates were placed on a clean glass surface, and dried. Typical fibrils were detected only in the solution that contained no substrates (h). Corresponding typical linear scans along the scan direction indicated in (g) and (h).

electron microscopy (JEOL, JEM 1010, Japan). Negative staining with uranyl acetate was used to visualize the aggregates.

RESULTS AND DISCUSSION

Large-sized tubular aggregates of Aβ40 on nano-Au surface were detected by AFM. The surfaces of the nano-Au after exposure to the Aβ40 solution were observed via AFM, which confirmed the presence of aggregated structures on the surface (Fig. 2(a)-(g)). While the typical diameters of previously reported fibrils [11] and those from the control experiment (Fig. 2(h)) did not exceed 10 nm, the height of the large tubular aggregates on the nanoparticles was determined to be 80-100 nm. It is noteworthy that the large-sized tubular aggregates of various lengths were in a stacked orientation on the nano-Au surface, i.e., present in the form of bundles. The surface coverage and the scale of the bundles increased with increasing incubation time. The AFM analysis of the nano-Au surface incubated with Aβ40, indicated the formation of abnormally large aggregates on the nano-Au surface. Although all images were obtained using the contacting mode of AFM, they exhibited a relatively clear, reproducible morphology. This suggests that the aggregates have a firm structure and bind strongly to the nano-Au surface. Small sizes and protofibrils of Aβ40 species were detected on the nano-Au surface. Absorbed protofibrils Aβ40 were present on the surface of nano-Au substrate after 12 hr, as evidenced by AFM analysis (Fig. 3(a)-(b)). Through the force-distance curves using the AFM, the presence of small sizes of Aβ40 species which may not be readily discerned by AFM was identified (Fig. 3(c)-(e)).

No evidence for the presence of large-sized tubular aggregates in solution was found. We also observed aggregation in solution, via AFM. Aliquots from the solution in the presence and absence of nano-Au substrates were placed on clean glass surfaces, and then dried. This method has been successfully used to image fibrillar and oligomeric structures that are formed in solution [13]. In the case of the control solution where Aβ40 was incubated in the absence of a nano-Au surface, typical fibrils were readily observed after 24 hr (Fig. 2(h)). However, no fibrils were observed after 24 hr exposure.

The adsorbed materials did not show a fibril-like morphology (data not shown), which indicates that they could be present as monomers or amorphous oligomers in the 24 hr exposed solution. This fact suggests that fibrillar growth of Aβ40 in the solution that had been exposed to the nano-Au surface was suppressed. The observed suppression of Aβ40 aggregation in the presence of gold substrates may be due to the depletion of Aβ40 in solution because of its binding to the gold substrates.

To examine the kinetics of this phenomenon in solution, ThT fluorescence assays as a function of incubation time were conducted in parallel with the morphological analyses (Fig. 4). Because ThT is used as a fluorescent probe for detecting fibrils and protofibrils, the fluorescence intensity can be taken as an estimate of the amounts

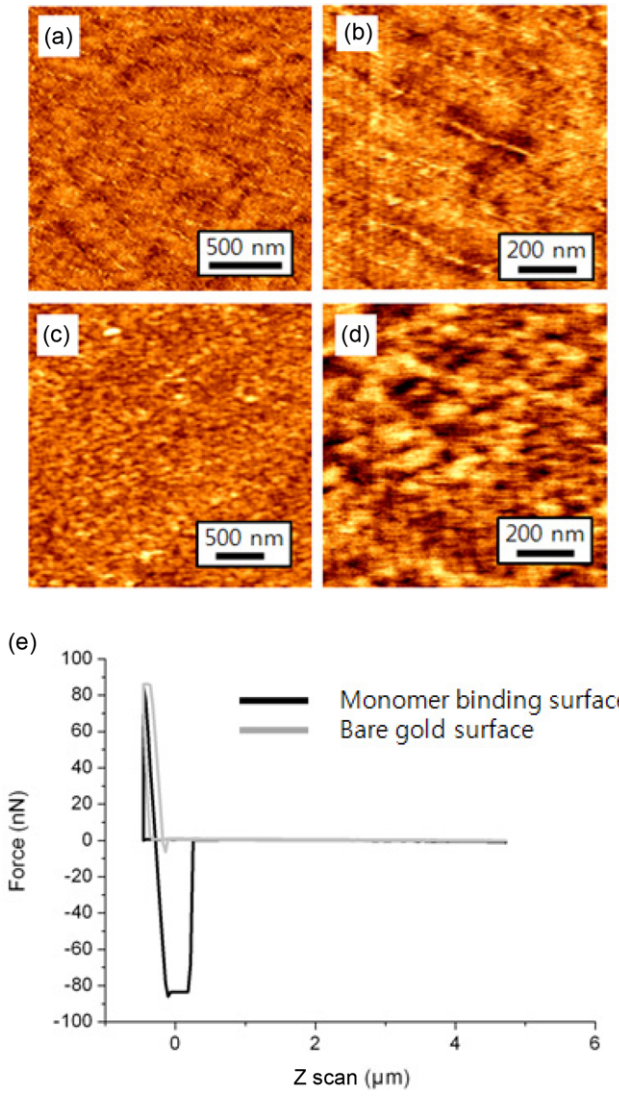

Fig. 3. AFM images of absorbed protofibrils (a)-(b) and monomers (c)-(d) of Aβ40 on a nano-Au surface; The incubation time in the Aβ40 solution was 24 hr. In order to confirm monomer binding, force-distance curves were obtained via AFM (e). The interaction between the AFM tip and the nano-Au surface exposed to Aβ40 can be clearly observed.

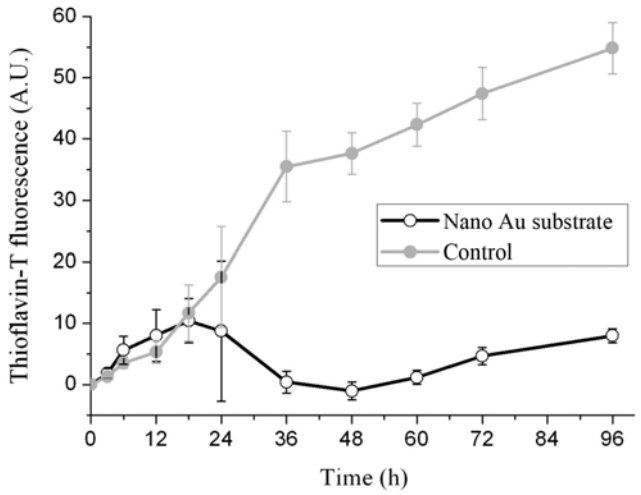

Fig. 4. Kinetics of the assembly of Aβ40 in solution in the presence (○) and absence (●) of a nano-Au surface. ThT fluorescence was plotted as a function of incubation time for 10 μM Aβ40 at 37 °C in PBS (pH 7.4) Averages and standard errors of the mean of four replicates are shown.

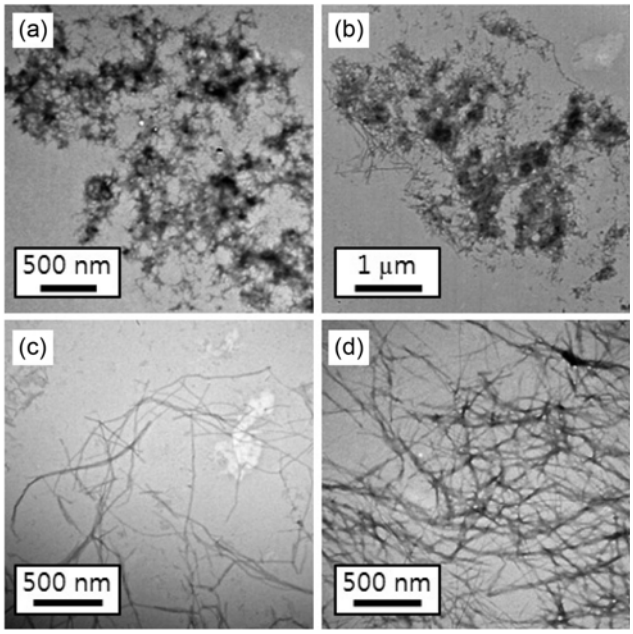

Fig. 5. TEM images of the Aβ40 aggregates in solution in contact with a nano-Au surface (a)-(c); Amorphous aggregates from the Aβ40 solution exposed to a nano-Au surface for 24 hr (a), partially fibril-like aggregates for 72 hr (b) and matured fibrils for 1 week were observed. In contrast, amyloid fibrils (d) were observed in the Aβ40 solution incubated for 24 hr in the absent of a nano-Au surface, i.e., in the control experiment.

present. The ThT intensity increased in the initial stage (0-18 hr), and a relatively large deviation in the range of 18-24 hr was found in both cases. After this, their ThT intensities showed a different tendency. In the case of the control solution, fibril formation proceeded normally, as evidenced by the continuous increase in fluorescence intensity. In contrast, the growth of fibrils in the solution that had been exposed to the nano-Au surface was suppressed. Namely, the intensity of the solution exposed the nano-Au surface was decreased for periods of up to 48 hr. However, subsequently, a moderate increase in intensity was found.

TEM analyses were performed to detect morphological changes in Aβ40 in solution. In the case of the control solution, typical fibrils were observed after a 24 hr incubation (Fig. 5(d)). However, from the solution-exposed nano-Au surface, only amorphous aggregates were found at the same incubation time of 24 hr (Fig. 5(a)). After 48 hr, some partially fibril-like aggregates appeared (Fig. 5(b)). However, while the fibril-like aggregates had an elongated shape, their length was shorter than the fibrils formed in the case of the control. In the solution that was incubated with a nano-Au surface for 1 week, typical fibrils with microsized lengths were also observed (Fig. 5(c)). The formation of abnormally large-sized aggregates as well as typical fibrils did not occur in the solution exposed to the nano-Au surface. It therefore appears that the abnormal assembly of Aβ40 takes place only on the nano-Au surface and the formed aggregates are not released into the solution by dissociation.

From the AFM results, the ThT biding assay and the TEM analysis, it can be concluded that the nano-Au surface participated in the formation of abnormally large tubular Aβ40 aggregates on their surface and inhibited formation of typical Aβ40 fibrils in solution. To explain the formation of these large-sized aggregates requires a mechanistic approach. Similar aggregates with a large size and elongated shape were reported in a previous study [14]. While our aggregates appeared after 3-4 days, however, they were incubated with Aβ for 70 days in the other study. In addition, incubation of the sonicated protein resulted in further aggregation, followed by the formation of large tangles of fibrillar aggregates. Based on our results, it is clear that abnormally large-sized assemblies are formed and typical fibril formation in solution is suppressed in the presence of a nano-Au surface. In addition, it is well known that the nature of the surface is a crucial factor in the formation of such an assembly including size, shape and the kinetics of formation, when the assembly of proteins occurs directly on a surface [9]. Various surfaces, including hydrophilic mica and hydrophobic graphite, have now been investigated [15]. However, the morphologies of the assemblies were not consistent with ours. A previous study reported that 'typical fibrillation' is unfavorable when Aβ40 is involved in tight interactions with suspended nanoparticles [8]. The findings reported herein suggest that interactions with nano-Au surfaces can lead to a larger scale of high local concentration states in the presence of a flat surface than suspended nanoparticles. Namely, while tight interactions between nanostructured surfaces and Aβ40 are unfavorable for typical fibril formation, such interactions may be appropriate for the formation of large-sized assemblies with nanostructured substrates. Although detailed mechanisms for the abnormal growth of Aβ40 have not yet been fully elucidated, the distinctive role of nanostructured substrates in the assembly of proteins is clearly striking.

The delayed fibril formation for the Aβ40 solution exposed to nano-Au surface can be explained by a decrease in the concentration of active monomers or protofibrils as the result of their adsorption to the nano-Au surface. It is noteworthy that the ThT intensity decrease starts at the time of formation of mature fibrils in the control batch. Our hypothesis is that the spontaneous structural change in Aβ40 drives the enhancement in binding affinity to the nano-Au substrates and the adsorbed Aβ40 serves as a starting material for formation of large-sized assemblies.

CONCLUSION

The effects of a nano-Au surface on the assembly of Aβ40 were investigated. The findings show that the nano-Au surface-associated with the assembly of Aβ40 led to the formation of abnormally large-sized tubular aggregates and the suppression of typical fibril formation in solution. In previous studies, in which suspended nanomaterials were used, large-sized aggregates consistent with our observations have not been reported. The binding of proteins to nanomaterials could lead to high local concentration nearby on their surface. A larger scale of high local concentration states along with a flatter surface than suspended nanoparticles could promote the abnormal assembly of Aβ40, followed by the formation of large sized tubular aggregates. This can be attributed to differences in the mechanism between immobilized and suspended nanomaterials. To develop nano-medications and assess the detrimental effects of nanomaterials with respect to proteins, this approach provides a basis for understanding nanomaterial-protein interactions on a nano-bio interface.

ACKNOWLEDGEMENT

This study was supported by the Ministry of Environment as "The Eco-Technopia 21" project. Authors appreciate the WCU (World Class University) program through the Korea Science and Engineering Foundation supported by the Ministry of Education, Science and Technology.

REFERENCES

1. I. Lynch and K. A. Dawson , *Nano Today*, **3**, 40 (2008).
2. J. Park, B. K. Kwak, E. Bae, J. Lee, K. Choi, J. Yi and Y. Kim, *Korean J. Chem. Eng.*, **26**, 1630 (2009).
3. V. L. Colvin and K. M. Kulinowski, *Natl. Acad. Sci. USA*, **104**, 8679 (2007).
4. S. Linse, C. Cabaleiro-Lago, W.-F. Xue, I. Lynch, S, Lindman, E. Thulin, S. E. Radford and K. A. Dawson, *Proc. Natl. Acad. Sci. USA*, **104**, 8691 (2007).
5. D. Zhang, O. Neumann, H. Wang, V. M. Yuwono, A. Barhoumi, M. Perham, J. D. Hartgerink, P. Wittung-Stafshede and N. J. Halas, *Nano Lett.*, **9**, 666 (2009).
6. W.-H. Wu, X. Sun, Y.-P. Yu, J. Hu, L. Zhao, Q. Liu, Y.-F. Zhao and Y.-F. Li, *Biochem. Bioph. Res. Co.*, **373**, 315 (2008).
7. C. Cabaleiro-Lago, F. Quinlan-Pluck, I. Lynch, S. Lindman, A. M. Minogue, E. Thulin, D. M. Walsh, K. A. Dawson and S. Linse, *J. Am. Chem. Soc.*, **130**, 15437 (2008).
8. K. Ikeda, T. Okada, S. Sawada, K. Akiyoshi and K. Matsuzaki, *FEBS Lett.*, **580**, 6587 (2006).
9. M. Zhu, P. O. Souillac, C. Ionescu-Zanetti, S. A. Carter and A. L. Fink, *J. Biol. Chem.*, **277**, 50914 (2002).
10. W. B. Jr. Stine, K. N. Dahlgren, G. A. Krafft and M. J. LaDu, *J. Biol. Chem.*, **278**, 11612 (2003).
11. C. Ha and C. B. Park, *Langmuir*, **22**, 6977 (2006).
12. T. Ban, D. Hamada, K. Hasegawa, H. Naiki and Y. Goto, *J. Biol. Chem.*, **278**, 16462 (2003).
13. E. M. Sigurdsson, *Amyloid proteins: Methods and protocols*, Humana Press, New Jersey (2005).
14. P. B. Stathopulos, G. A. Scholz, Y.-M. Hwang, J. O. Rumfeldt, J. R. Lepock and E. M. Meiering, *Protein Sci.*, **13**, 3017 (2003).
15. T. Kowalewski and D. M. Moltzman, *Proc. Natl. Acad. Sci. USA*, **96**, 3688 (1996).